Biological dose calculation on dual-layered DECT images for CIRT

2021 Spring KNS

Euntaek Yoon, Seongmoon Jung, Jaeman Son,
Bitbyeol Kim, Chang Heon Choi, Jung-in Kim, Jong Min Park

xmfla0803@gmail.com
Institution of Radiation Medicine
Seoul National University Medical Research Center, Republic of Korea

SNUH 서울대학교병원 SEOUL NATIONAL UNIVERSITY HOSPITAL

Contents

I. Introduction

Ion therapy

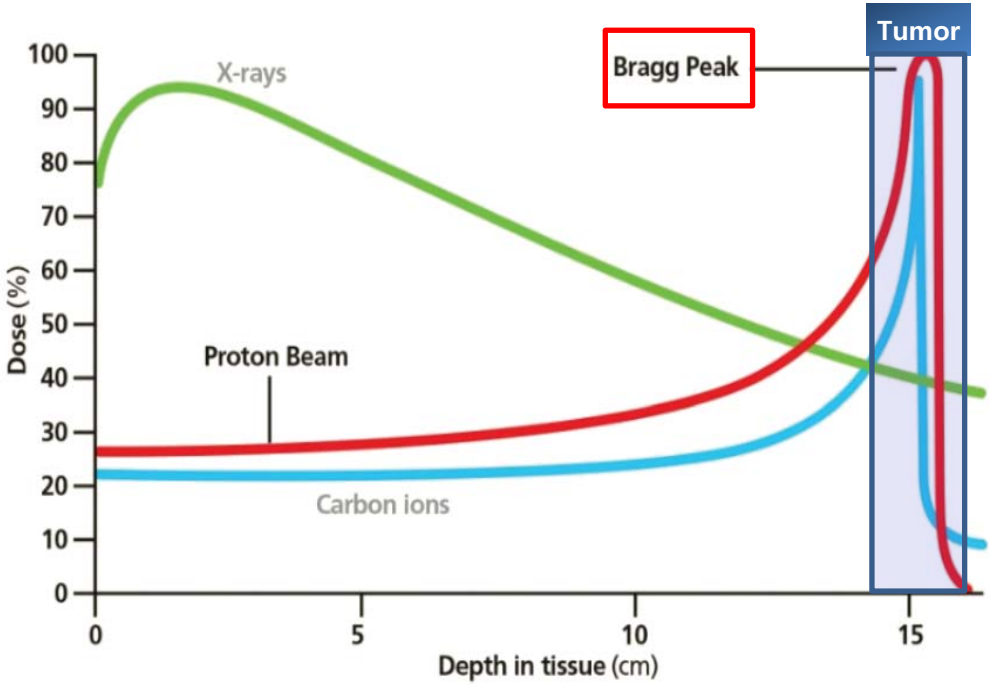

B. Mustapha, et al. 2016

Bragg peak

- Reduction of exposure to normal tissues

Ion therapy

- proton, **Carbon**, α-particles, ions

I. Introduction

Proton therapy

Range Uncertainty exists (2012, paganetti)

- Organ motion, setup and anatomical variation, dose calculation approximation, biological consideration
- Range margin : 3.5 % + 1 mm (MGH)

  ex) 20 cm range field → 8 mm margin

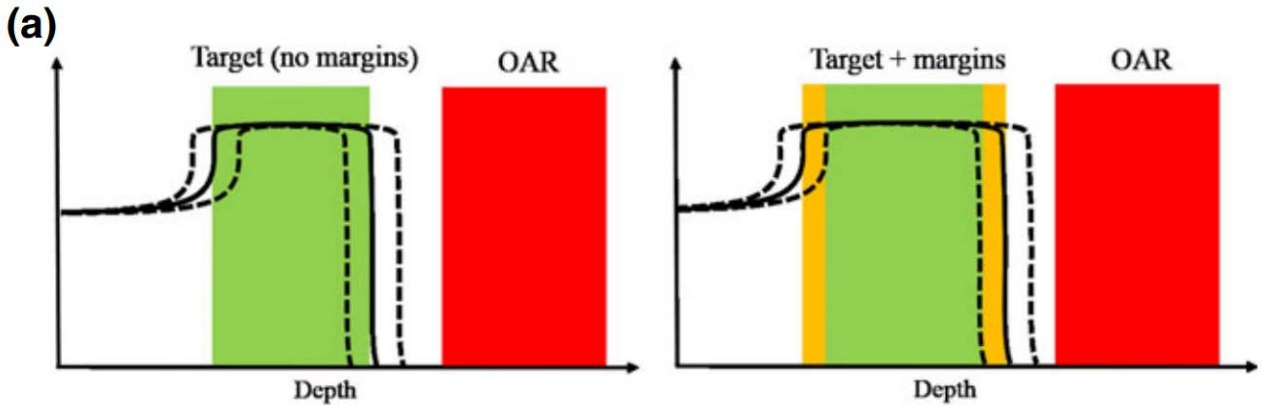

E. Bar, et al. 2017

I. Introduction

Carbon ion therapy

Difference with proton therapy

- larger **Relative Biological Effectiveness (RBE)**

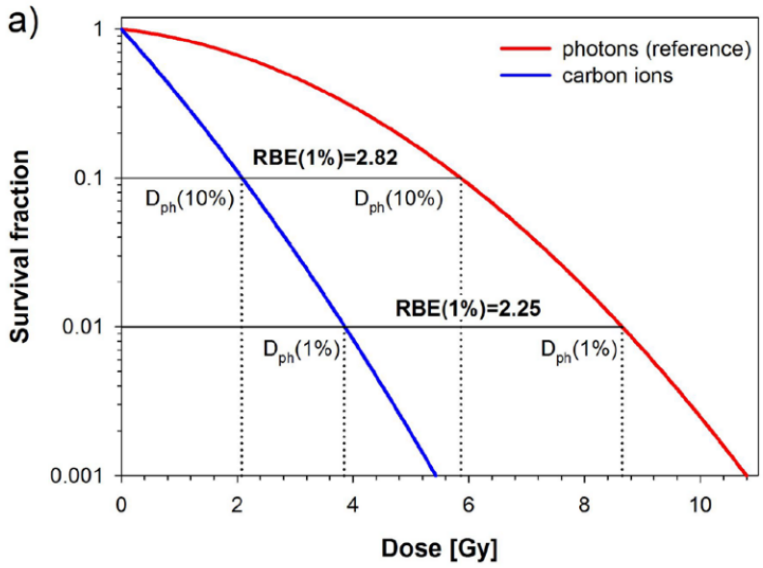

Karger, et al. 2017

$$\mathrm{RBE} = \left.\frac{D_{\mathrm{ph}}}{D_{\mathrm{ion}}}\right|_{\mathrm{isoeffect}}$$

☞ **Biological dose** (BD) =
RBE × Physical dose

Carbon Ion Treatment planning is based on **biological dose**

I. Introduction

For successful carbon ion treatment?

Accurate Dose calculation

Monte Carlo simulation

Reduction of range uncertainty

→ **Dual energy CT (DECT)**

I. Introduction

Research purpose

- Calculation of biological dose in CIRT using DECT image using Monte Carlo simulation

- Comparison of DECT-based and SECT-based dose calculation results

II. Method

* HU : Hounsfield unit, CT number

DECT vs SECT

DECT

HU_H, HU_L → Z_{eff} , ρ_e → Material RSP

SECT

HU → Material RSP

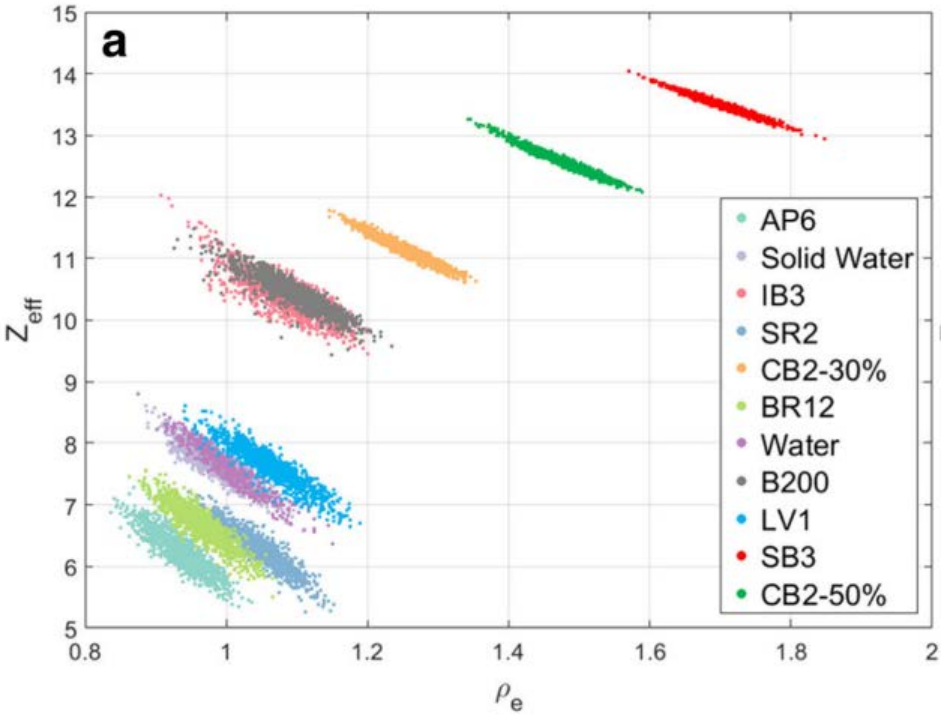

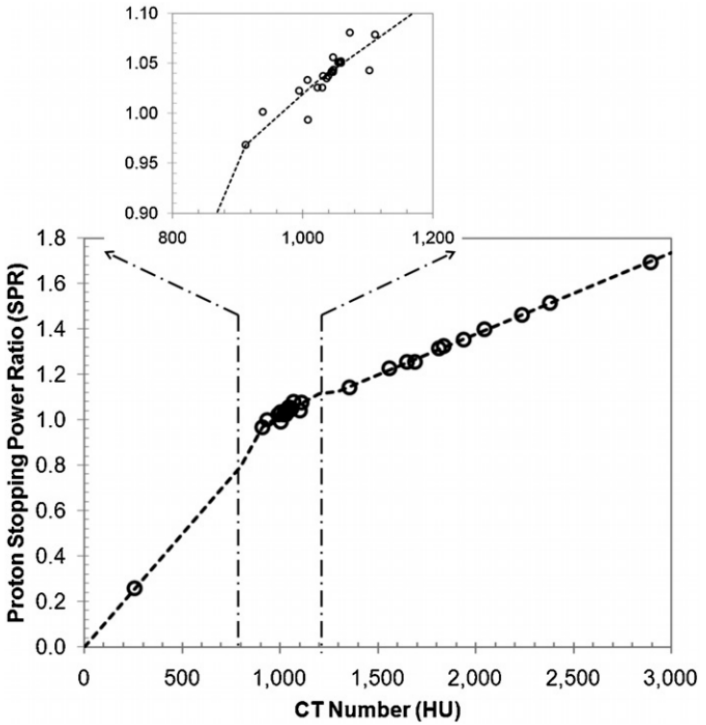

Vaniqui, et al. 2017

II. Method

Dual-layered DECT

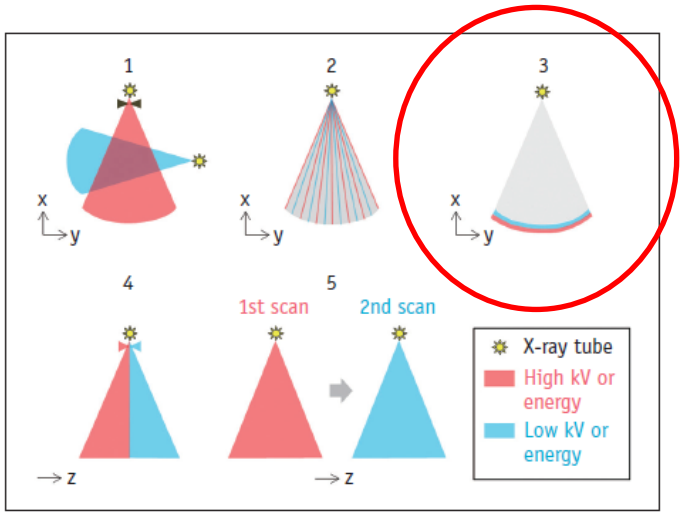

Fig. 1. Illustration of five different methods of dual-energy CT data acquisition. 1 = dual tubes with or without beam filtration, 2 = rapid voltage switching with single tube, 3 = dual-layer detector with single tube, 4 = single tube with split filter, 5 = single tube with sequential dual scans

Goo et al, *Korean J Radiol*, 2017

Philips, IQon spectral CT

Advantages

- Real time
- offers Virtual Monochromatic Image
- Retrospective DECT analysis **(offers Z_{eff}, ρ_e)**

Disadvantages

- lower sensitivity to optical photon
- cross-talk between the two detector layers

II. Method

RBE Calculation model

Local Effect Model (LEM)

$$\overline{N(D)} = \int \frac{-\ln S\left(d\left(x,y,z\right)\right)}{V} \mathrm{d}V.$$

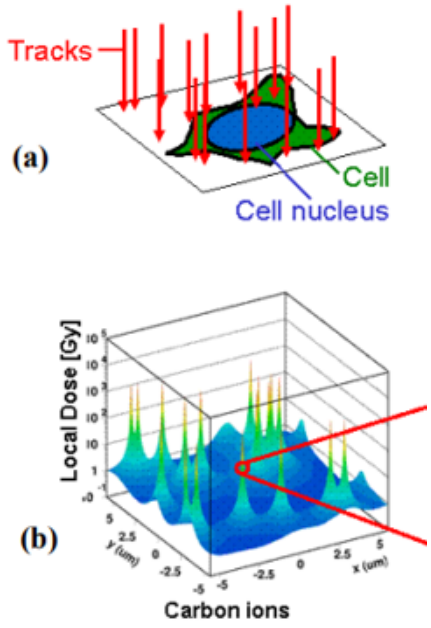

Friedrich, 2013

Microdosimetric Kinetic model (MKM)

$$\overline{N(D)} = -\ln S = (\alpha_0 + \beta z_{1D}^{*})D + \beta D^2$$

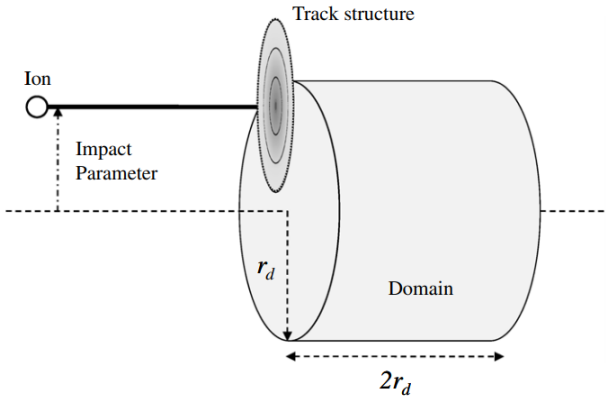

Figure 1. Schematic of an incident ion with respect to a cylindrical sensitive volume.

II. Method

MKM model

Modified MKM(mMKM)(2010, inaniwa)

$$\overline{N(D)} = -\ln S = (\alpha_0 + \beta z^*_{1D})D + \beta D^2$$

α_0 = 0.172, β = 0.0615 (constant)
z^*_{1D} : Dose mean saturation corrected **specific energy in domain**

	Reference	This study
Micro	Track structure model	Monte Carlo simulation (**TOPAS**, geant4-dna)
Macro	Monte Carlo simulation (Geant4)	Monte Carlo simulation (**TOPAS**, QGSP_BIC_HP)

II. Method

Microdosimetric simulation

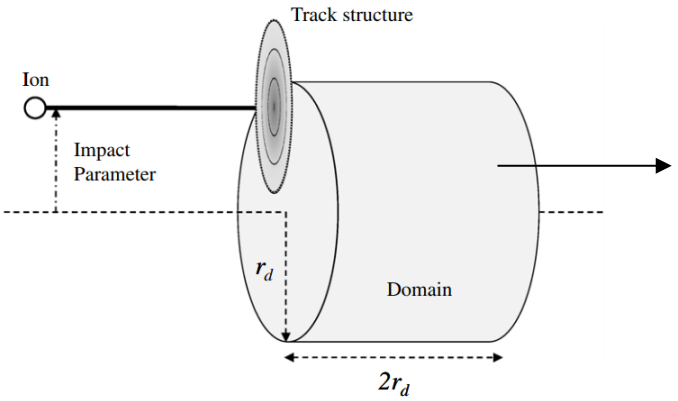

Z (specific energy)

Inaniwa, 2010

Figure 1. Schematic of an incident ion with respect to a cylindrical sensitive volume.

Reference (2010, Inaniwa)

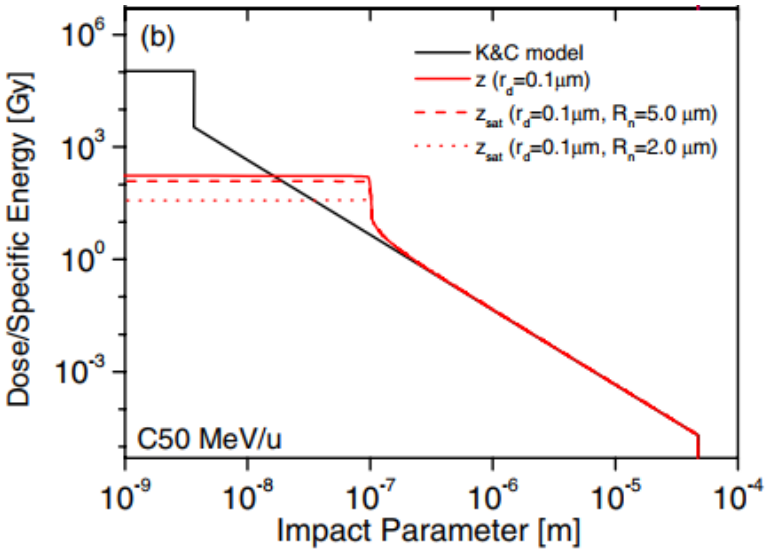

TOPAS simulation result

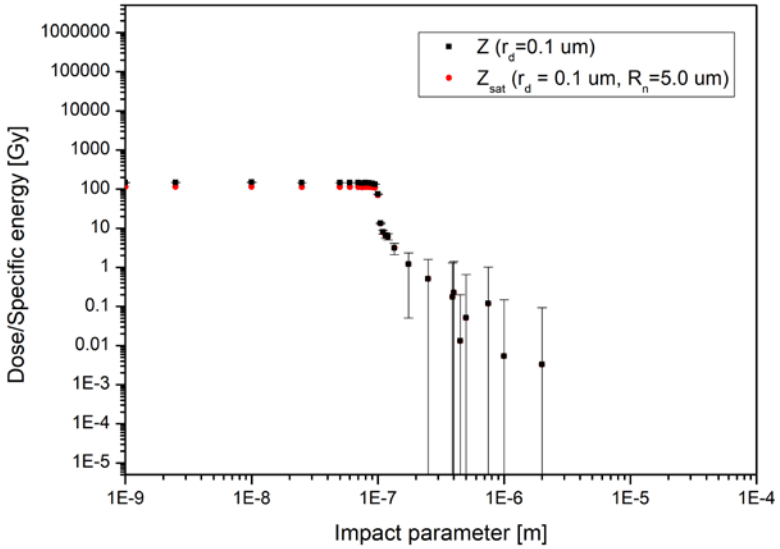

II. Method

Schematic diagram of B.D calculation process

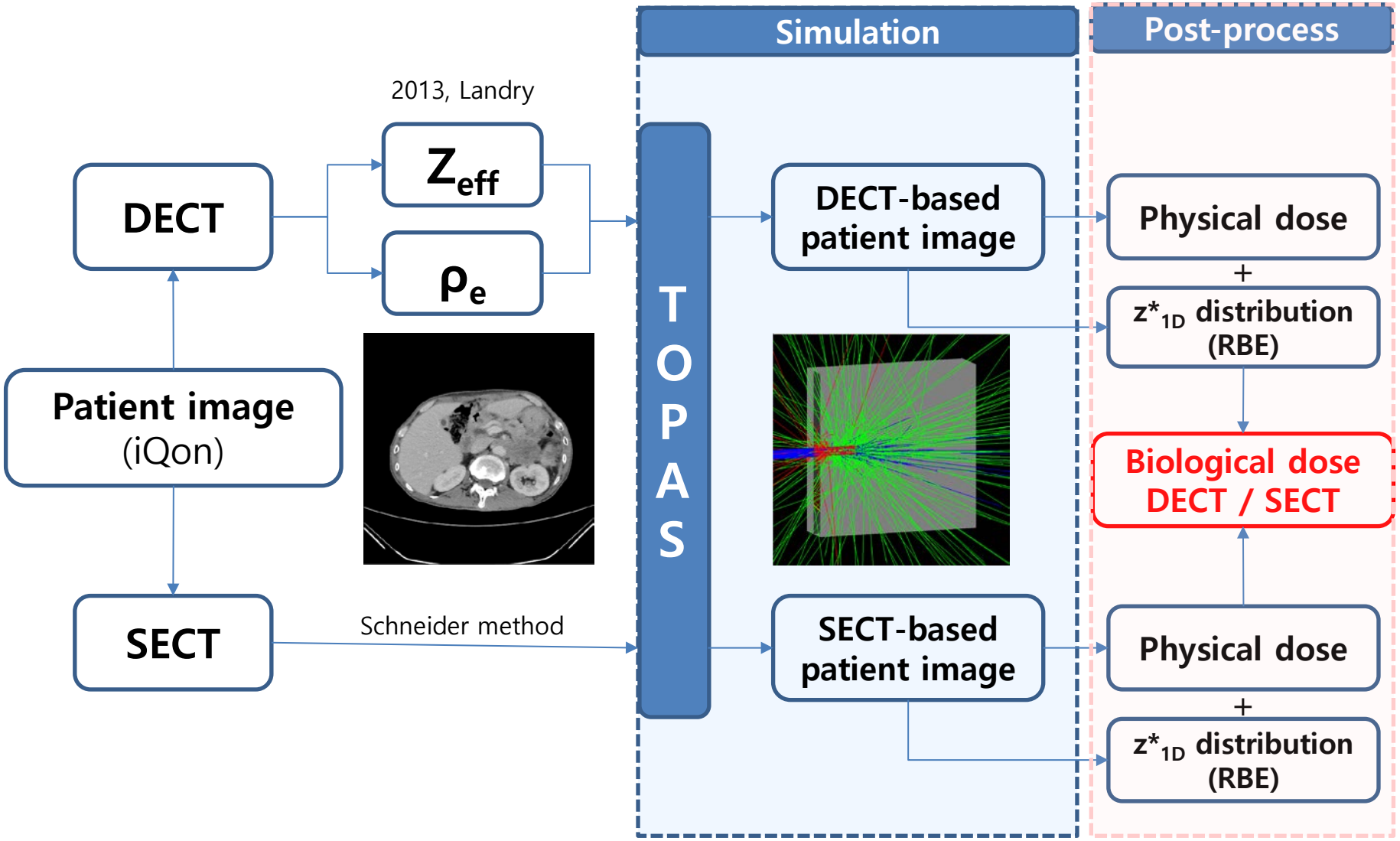

II. Method

TOPAS simulation

① Abdomen (soft tissue) : pancreas + partial abdomen

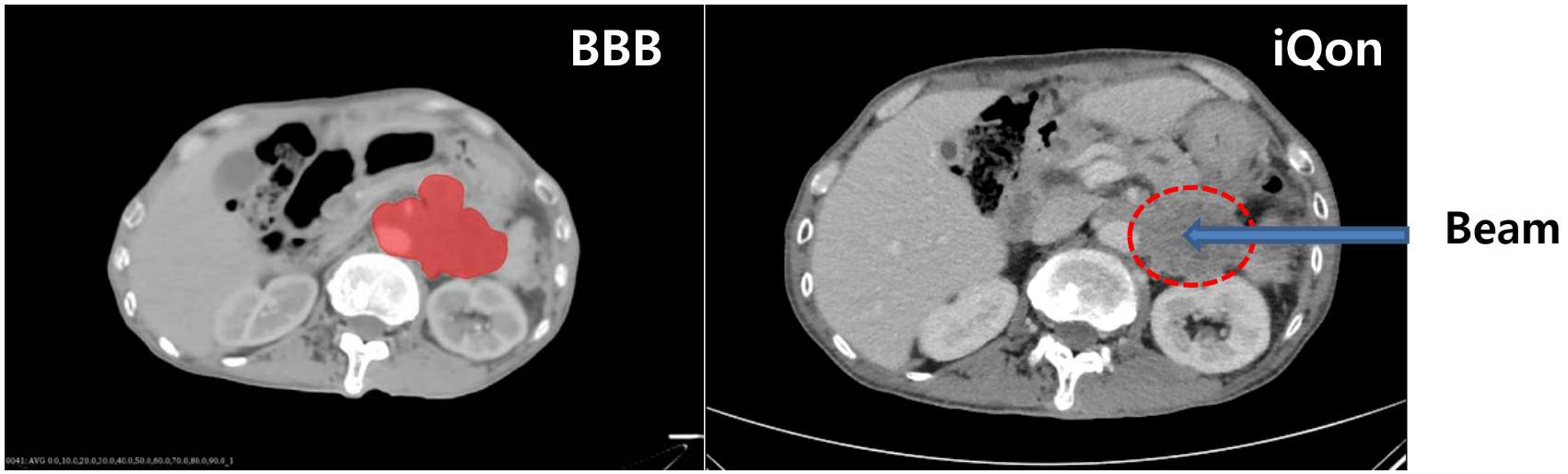

Beam specification : monoenergetic , 180 MeV/u , σ = 3 mm
History : 10^5 / Scoring z*1D simultaneously

II. Method

TOPAS simulation

② Head and Neck (bone) : sternum

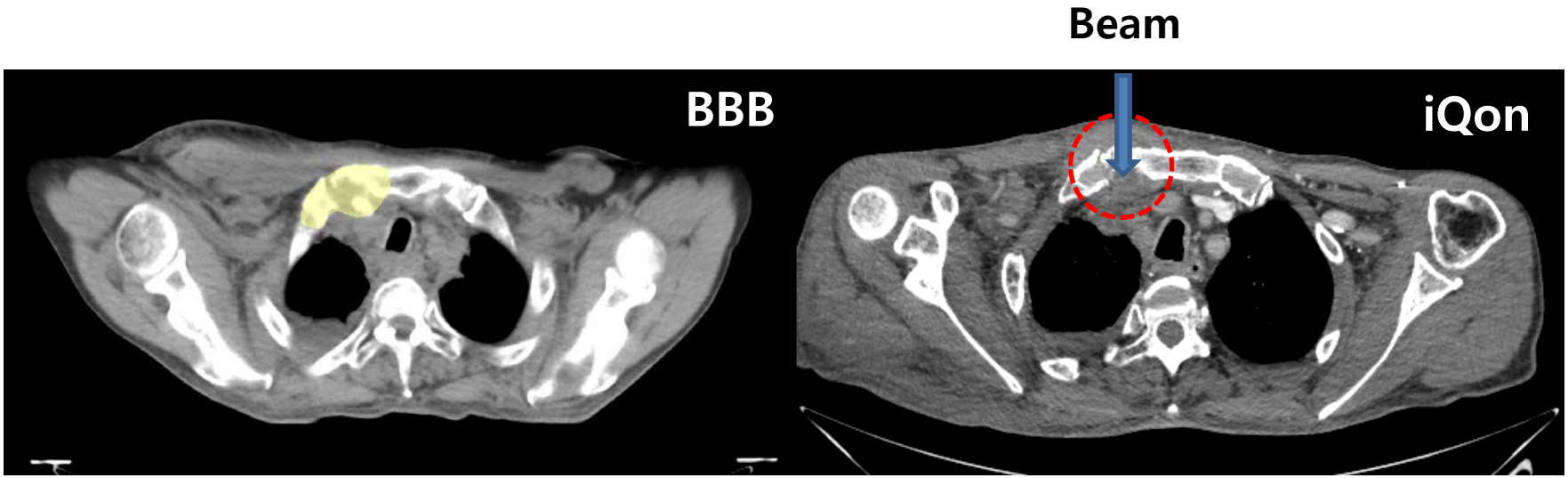

Beam specification : monoenergetic , 130 MeV/u , σ = 3 mm
History : 10^5 / Scoring z*1D simultaneously

III. Results

Specific energy (z^*_{1D}) table

Inaniwa (2010)

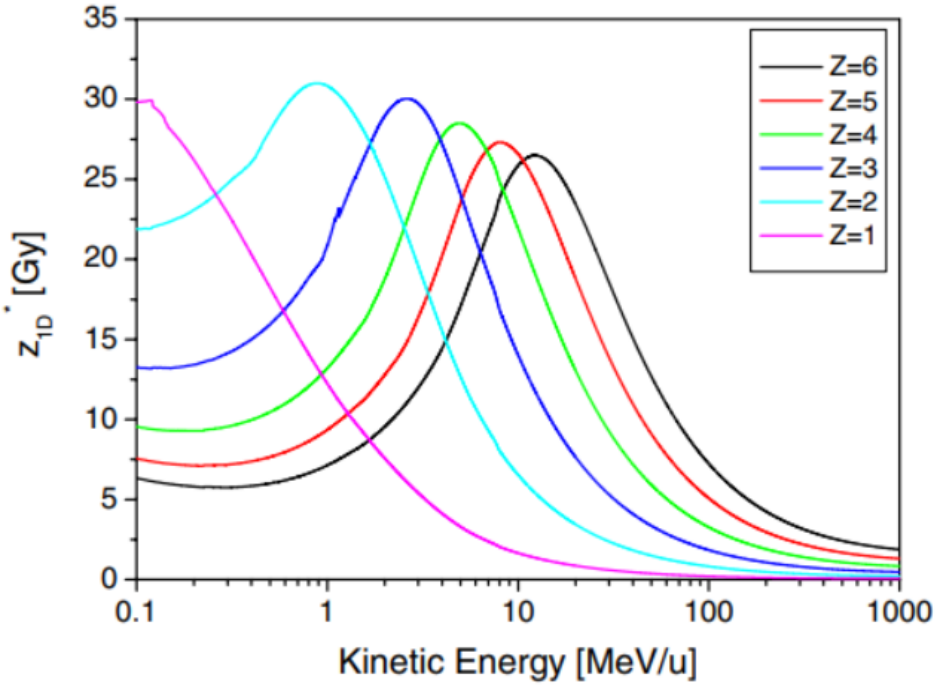

Analytical model based calculation

TOPAS microdosimetric simulation

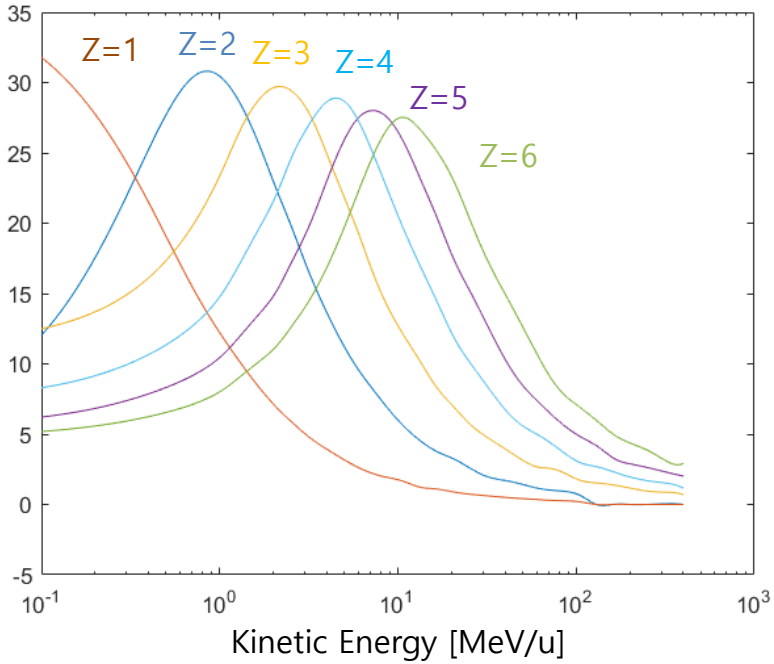

Monte carlo calculation

III. Results

Physical dose distribution

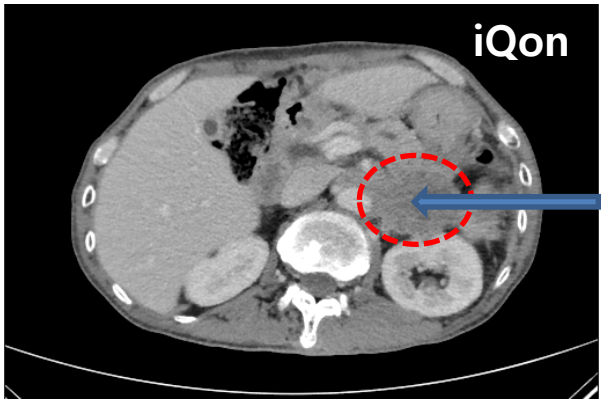

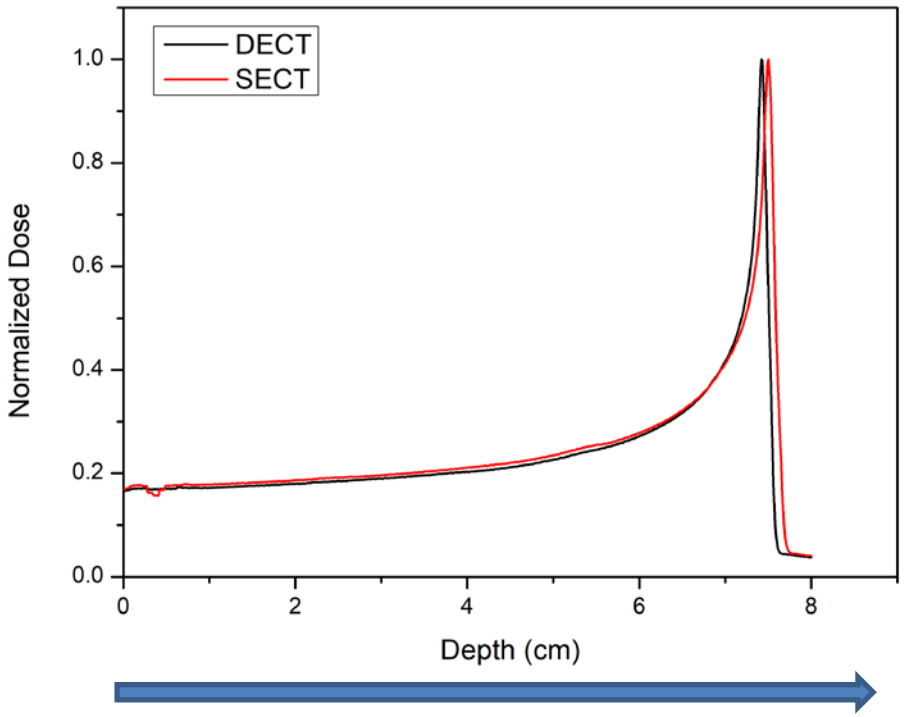

Range(R_{80}) difference : 0.8 mm, 1.1 %

※ R_{80} : depth of the 80% distal end of the Bragg peak maximum

III. Results

Physical dose distribution

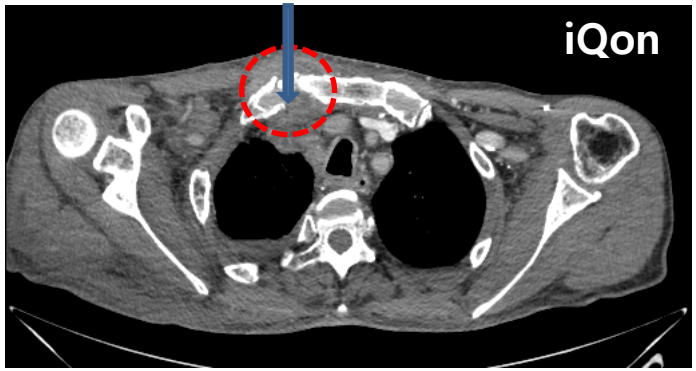

For head and neck patient

Range(R_{80}) difference : mm

III. Results

z^*_{1D} distribution

Abdomen patient

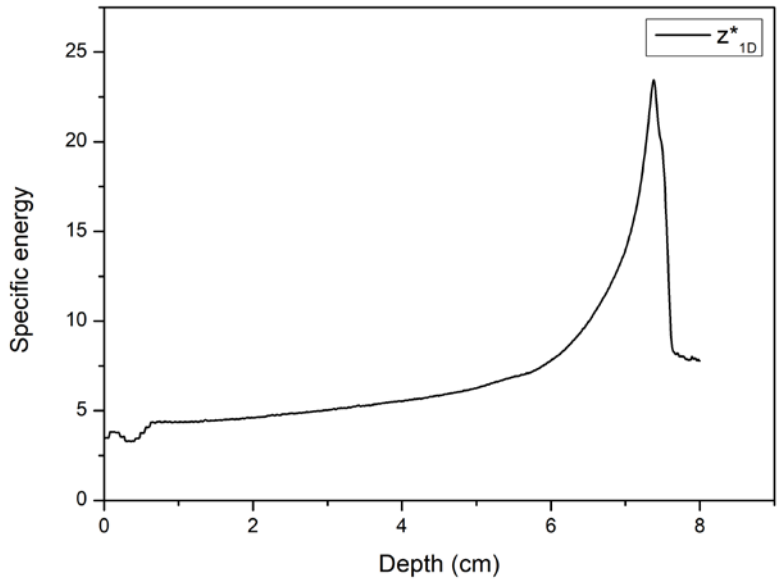

H&N patient

For head and neck patient

Common to DECT / SECT

III. Results

Biological dose distribution

Normalized by biological dose : 4.4 Gy (RBE)

For pancreatic cancer patient, Carbon-ion Radiotherapy, 2014

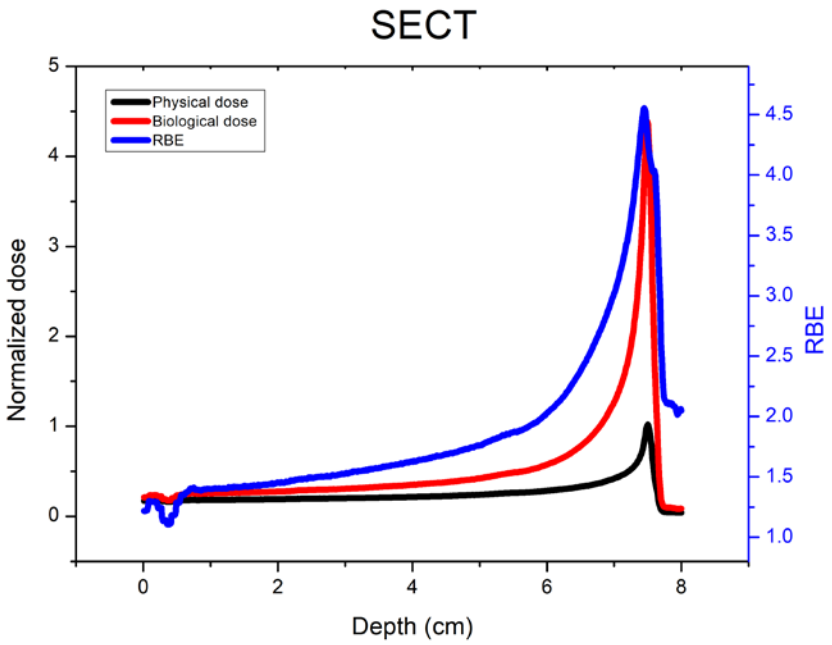

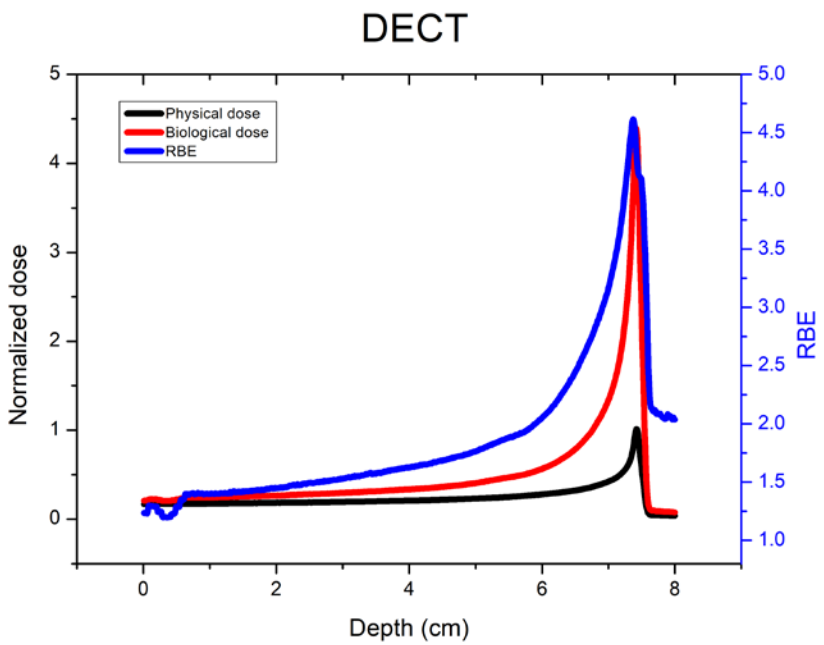

Normalized physical dose difference : 0.5 %

III. Results

Biological dose distribution

Normalized by biological dose : Gy (RBE)

For sternum cancer patient, Carbon-ion Radiotherapy, 2014

For head and neck patient

For head and neck patient

Normalized physical dose difference : %

4. Discussion & Conclusion

- By applying DECT, which can reduce the intrinsic uncertainty of SECT-based calculation, DECT-based biological dose calculations for patients were performed through Monte Carlo simulations.

- In addition, SECT-based dose calculation was performed and the results were compared in two patient case.

- In the soft tissue of the abdomen, the range difference was 0.8 mm (1.1 %) and in the H&N patients containing bone, the range was xx mm (yy %).

- The difference between the physical dose at the target internal point was calculated based on the DECT and SECT-based biological dose calculation results, and it was found to be 0.5% in soft tissue and zz% in tissue containing bone.

- If DECT is used in place of SECT through further verification, it is expected that correction of the range uncertainty will be greater in the area containing bone than in the area containing a lot of soft tissue.

Thank you for attention